ISBN: 978-3-95450-262-2 ISSN: 2673-5350 doi: 10.18429/JACoW-IBIC2025-WEPMO33

STUDIES OF LONGITUDINAL PHASE SPACE TOMOGRAPHY USING BOOSTER CAVITY AND DIPOLE SPECTROMETER

G. Kim, M. Chung*, Pohang University of Science and Technology, Pohang, South Korea
D. Kwak, Korea Atomic Energy Research Institute, Jeonbuk, South Korea

Abstract

Information on the longitudinal phase space (LPS) is essential for tuning injectors that deliver 0.1-1 ps electron bunches to beam-plasma interaction experiments and ultrafast diffraction facilities. Instead of relying on specialized diagnostics, we demonstrate that LPS characterization can be achieved using only standard accelerator components, namely a booster cavity and a downstream spectrometer. A phase scan of the booster cavity adjusts the longitudinal chirp, while the spectrometer converts the energy spread into a transverse distribution. In particular, particle tracking simulations show that by applying the simultaneous algebraic reconstruction technique (SART). We obtained the reconstruction image less than 5 % error. Next, we are planning to discuss the potential application of LPS tomography developed to non-relativistic ion beams, using a re-bunching cavity and a bunch shape monitor.

MOTIVATION

Precise LPS characterization is critical for optimizing ultrafast electron bunch injectors in beam-plasma interaction experiments and ultrafast diffraction facilities. These applications demand a 0.1-1 ps electron bunches with precisely tailored temporal profiles, making LPS diagnostics an essential component of injector tuning protocols [1, 2].

The core idea lies in applying reconstruction algorithms to indirectly measure LPS through phase scan data. By varying the booster cavity phase, we generate different longitudinal chirp conditions that, when combined with dipole spectrometer measurements, provide required information for complete LPS reconstruction using the SART.

TOMOGRAPHY DATA PREPARATION, AND MODELLING

Workflow Overview

We follow a four-step workflow for LPS tomography: (1) acquire 1D projections by scanning the booster cavity phase; (2) map each phase to an rotation angle in the $(\varphi, \delta p)$ plane; (3) pre-process each profile (background subtraction, and normalization); and (4) reconstruct the LPS using an iterative algorithm. Accurate 1D projections and sufficiently uniform angle coverage are the two key factors of high-accuracy reconstruction.

Simulation Setup

The reconstruction validation was performed using comprehensive particle tracking simulations implemented in ASTRA (A Space Charge Tracking Algorithm) [3]. The simulation was configured to represent our beamline (see Fig. 1), called the electron Linear Accelerator for Basic science (eLABs) (see Table 1).

Table 1: The Beamline Parameters

Parameters	Specifications
Energy	70 MeV
Charge	200 pC
The number of particles	100,000
Space charge	OFF
Bunch length	1.2739 ps
Phase increment	0.1 deg

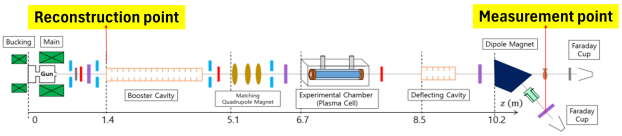

Figure 1: Our beamline can accelerate the beam up to 70 MeV. To reconstruct gun LPS image, reconstruction point is upstream of booster cavity, whereas the measurement point is after the spectrometer.

Physical Model

We neglect space charge in the initial validation because the analytical relations used for angle mapping do not include space charge. For the ultra-relativistic, bunch length is sufficiently conserved through the booster and transport to the spectrometer [4]. So, we assume the bunch length is constant between reconstruction point and measurement point.

Under these assumptions, the longitudinal dynamics across the booster can be written as [5]

$$p_z^{\mathrm{boo}} = p_z^{\mathrm{gun}} + S\,\delta\varphi + \delta p + V\cos(\varphi + \delta\varphi). \qquad (1)$$

Eq. (1) decomposes the p_z^{boo}, into the upstream momentum p_z^{gun}, a linear transport term $S\,\delta\varphi$ capturing longitudinal chirp according to bunch length, an uncorrelated energy jitter δp, and the RF acceleration term $V\cos(\varphi + \delta\varphi)$.

$$\langle p_z^{\mathrm{boo}} \rangle \approx p_z^{\mathrm{gun}} + V\cos\varphi\left(1 - \frac{\sigma_\varphi^2}{2}\right). \qquad (2)$$

Eq. (2) is a second-order expansion of the mean momentum. In practice, we fit the measured mean momentum versus booster phase to extract an effective gain V and to confirm the on-crest phase φ_0.

* moses@postech.ac.kr

ISBN: 978-3-95450-262-2 ISSN: 2673-5350 doi: 10.18429/JACoW-IBIC2025-WEPMO33

$$\sigma_p^2 = \sigma_{p,\min}^2 + (V\sigma_\varphi)^2(\sin\varphi - \sin\varphi_{\sigma_{p,\min}})^2. \quad (3)$$

Eq. (3) models the projected momentum spread versus phase, where $\sigma_{p,\min}$ is the minimum uncorrelated spread reached at phase $\varphi_{\sigma_{p,\min}}$.

Using Eqs. (2) and (3), we compare model with the simulation (see Fig. 2). The left panel determines the reference operating phase via the gun scan, and the right panel shows the booster phase scan with model overlays used to calibrate V, $\sigma_{p,\min}$, and $\varphi_{\sigma_{p,\min}}$.

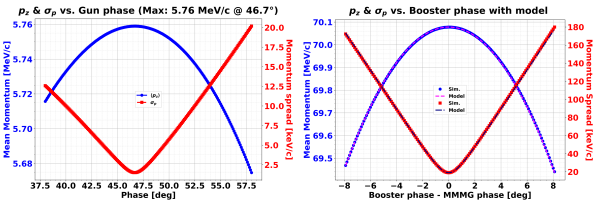

Figure 2: Phase scan results from both gun and booster cavity. (Left) Gun phase scan to define the reference operating point; (Right) Booster phase scan with model fits for mean and spread.

These expressions provide checks between simulation and the model, and supply the parameters required to assign a phase advance Φ to each booster cavity phase step.

$$\sigma_\varphi \approx \frac{\sigma_p}{|V\sin\varphi|}. \quad (4)$$

Combining Eqs. (2) and (3) yields a closed-form $\sigma_\varphi(\varphi)$ used for angle mapping; the resulting bunch-length trend is shown in Fig. 3 (left). The phase advance Φ is given by [5]

$$\Phi = \tan^{-1}\left(\frac{S\sigma_\varphi}{\sigma_{p,\min}}\right), \quad (5)$$

where S is the longitudinal chirp and $\sigma_{p,\min}$ is the minimum projected spread over the scan.

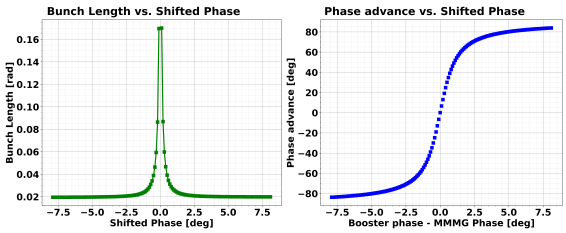

Figure 3: Modelled beam parameters versus the shifted booster phase. (Left) Bunch length σ_φ; (Right) Phase advance Φ from Eq. (5).

Figure 3 (right) shows this phase advance curve, i.e., the mapping from booster cavity phase to the rotation angle. With this, we obtained the complete set of projection angles corresponding to the projection, enabling direct application of tomography to the measured profiles.

Reconstruction Algorithm: SART

We employed SART method for LPS reconstruction, which is well-known for its stable convergence properties. A key advantage of SART is its resistance to stripe noise [6]. By updating the image using data from all projection angles simultaneously in each iteration, SART effectively averages out and suppresses artifacts. Additionally, SART converges to a accurate solution in a few iterations [6]. The algorithm is described by [5]

$$\vec{x}^{(k+1)} = \vec{x}^{(k)} + \frac{1}{\vec{A}^\top 1} \cdot \frac{(\vec{m} - \vec{A}\,\vec{x}^{(k)})}{\vec{A}^\top 1}. \quad (6)$$

$\vec{x}^{(k)}$ is the image estimate at the k-th iteration, while $\vec{x}^{(k+1)}$ is the updated image for the next iteration. The vector $\vec{m}$ contains the measured projection data (i.e., the sinogram), and $\vec{A}$ is the weight matrix that models the linear forward projection ($\vec{A}\vec{x}$). The expression $(\vec{m} - \vec{A}\vec{x}^{(k)})$ calculates the residual, which is the difference between the sinogram and predicted.

SIMULATION RESULTS

We used the scikit-image library to apply tomography algorithm. We took the sinogram and used SART method with initial estimate as uniform values.

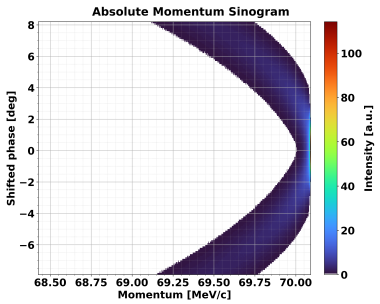

Figure 4: Projected momentum distribution versus booster cavity phase.

Figure 4 shows the sinogram which is the projected momentum distribution according to booster cavity phase. The central region around the Maximum Mean Momentum Gain (MMMG) exhibits the highest intensity, while the projected momentum spread increases as the phase far away from MMMG phase.

To examine how phase advance coverage impacts reconstruction, we reconstruct the LPS with 50° and with the full angle sets using identical settings (see Fig. 5, 6). The full-range can reconstruct the tail of bunch better than the 50°. The quantitative trend in Fig. 7 shows an optimum near about 80°.

Compensating Algorithm-Induced Artifacts

Limited range and non-uniform spacing can introduce noise to iterative tomography. From Fig. 3, Φ is not uniform over the full range, which over-weights certain projections. We therefore:

ISBN: 978-3-95450-262-2 ISSN: 2673-5350 doi: 10.18429/JACoW-IBIC2025-WEPMO33

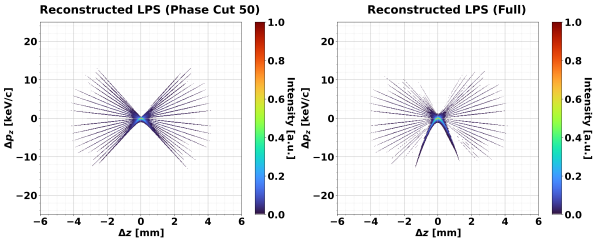

Figure 5: The dependency of reconstruction quality on the selected range. (Left) Reconstruction within 50°; (Right) Reconstruction using all phase advance. Estimated bunch length is about 1.17 mm, which is quite larger than the ground truth (0.327 mm).

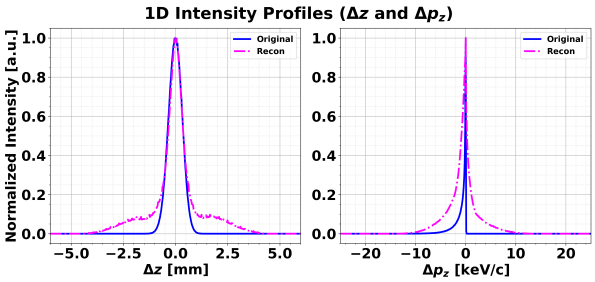

Figure 6: 1D profiles of reconstructed LPS from whole phase advance range. The blue line is the original profile from ASTRA simulation, and the magenta line is the reconstructed profile from tomography algorithm. (Left) Longitudinal bunch length profile; (Right) Momentum distribution profile.

- Investigate the dependency of a phase advance range: exclude unevenly spaced phases (see Fig. 7).
- Trim low-signal tails in each profile with a charge cut to suppress algorithm's artifacts.

Figure 7(a) shows that performance improves as unevenly spaced angles are excluded, with an optimum in our case near a 80° range. Applying a 2.2 % charge cut suppresses artifacts. Figure 7(b) confirms that the reconstructed 1D profiles follow the ground truth across the core while reducing artifacts.

Figure 8 compares the ground-truth with the final optimized image. The ground-truth (left), generated via ASTRA simulation, serves as the reference for validating the algorithm. The optimized image (right) is obtained using a 80° phase advance range and a 2.2 % charge cut. These result effectively suppress artifacts. The final reconstruction preserves the longitudinal profiles of the bunch, demonstrating the feasibility of the LPS. The bunch length of optimized LPS has 0.338 mm, while initial estimation was 1.17 mm, and the ground truth has 0.327 mm. The optimized reconstruction yields a bunch length error of less than 5 %, significantly better than the initial estimation, demonstrating the effectiveness of artifact compensation strategies.

SUMMARY AND OUTLOOK

We validated a LPS tomography using ASTRA and an analytical model, and SART-based reconstruction recover

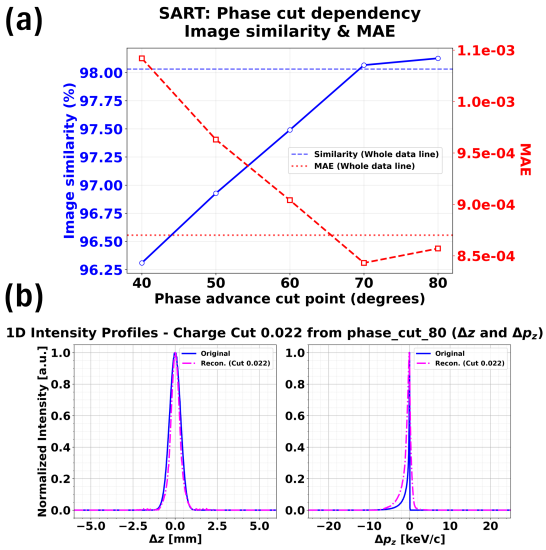

Figure 7: (a) SART performance versus phase advance cut (higher image similarity and lower MAE are better). (b) 1D profiles at the selected range using a 80° range and a 2.2 % charge cut; blue: ground truth, magenta: reconstruction.

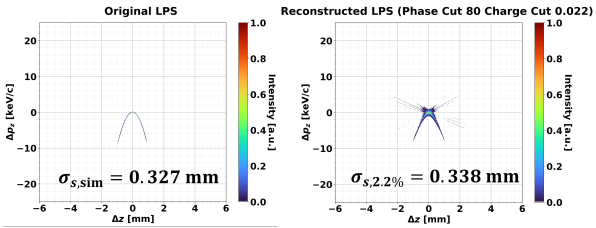

Figure 8: (Left) The simulation result from ASTRA. This is treated as the ground truth for validating the tomography algorithm., (Right) Optimized LPS reconstruction using a 80° phase advance range and a 2.2 % charge cut.

the LPS with an error of about 5 %, while artifact compensation via a restricted phase advance range, and a charge cut, yielding profiles that closely match simulation. For future work, we plan to refine a weight matrix $\vec{A}$ with further data analysis. We will extend the study to characterize few-femtosecond bunches and validate the reconstructions against direct measurements from an RF deflecting cavity. Finally, we will discuss the potential application of this method to non-relativistic ion beams.

ACKNOWLEDGEMENTS

This work was supported by the National Research Foundation of Korea (NRF), funded by the Ministry of Science and ICT of the Republic of Korea (RS-2022-00154676 and RS-2022-00214790).

REFERENCES

[1] D. Dowell *et al.*, "Longitudinal emittance measurements at the SLAC gun test facility", *Nucl. Instrum. Methods Phys. Res.*

ISBN: 978-3-95450-262-2 ISSN: 2673-5350 doi: 10.18429/JACoW-IBIC2025-WEPMO33

A, vol. 507, no. 1, pp. 331–334, 2003. doi:10.1016/S0168-9002(03)00940-9

[2] H. Loos *et al.*, "Longitudinal phase space tomography at the SLAC gun test facility and the BNL DUV-FEL", *Nucl. Instrum. Methods Phys. Res. A*, vol. 528, no. 1, pp. 189–193, 2004. doi:10.1016/j.nima.2004.04.044

[3] K. Floettmann, *A space charge tracking code – ASTRA*, Deutsches Elektronen-Synchrotron DESY. http://www.desy.de/~mpyflo

[4] D. Malyutin *et al.*, "Longitudinal phase space tomography using a booster cavity at PITZ", *Nucl. Instrum. Methods Phys. Res. A*, vol. 871, pp. 105–112, 2017. doi:10.1016/j.nima.2017.07.043

[5] N. Aftab, "4D transverse and 2D longitudinal phase space characterization of high brightness electron beams at PITZ", Work performed at DESY/PITZ, Zeuthen, Ph.D. thesis, Fachbereich Physik, Universit"at Hamburg, Hamburg, Germany, 2024.

[6] P. C. Hansen, J. Jørgensen, and W. R. B. Lionheart, *Computed Tomography: Algorithms, Insight, and Just Enough Theory*. Philadelphia, PA, USA: Society for Industrial and Applied Mathematics, 2021. doi:10.1137/1.9781611976670